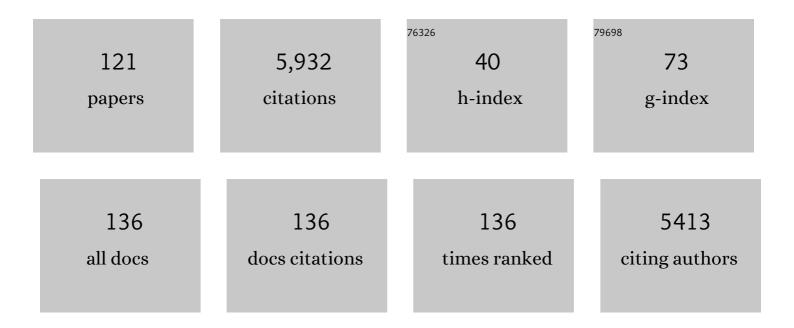
## Sascha Ott

List of Publications by Year in descending order

Source: https://exaly.com/author-pdf/3205373/publications.pdf Version: 2024-02-01



#	Article	IF	CITATIONS
1	Investigation of the heat distribution in dry friction systems during fade and recovery using fiber-optic sensing and infrared technology. Friction, 2022, 10, 422-435.	6.4	6
2	Electrocatalytic water oxidation from a mixed linker MOF based on NU-1000 with an integrated ruthenium-based metallo-linker. Materials Advances, 2022, 3, 4227-4234.	5.4	3
3	Hydroxyl-Decorated Diiron Complex as a [FeFe]-Hydrogenase Active Site Model Complex: Light-Driven Photocatalytic Activity and Heterogenization on Ethylene-Bridged Periodic Mesoporous Organosilica. Catalysts, 2022, 12, 254.	3.5	4
4	Microscopic Insights into Cation-Coupled Electron Hopping Transport in a Metal–Organic Framework. Journal of the American Chemical Society, 2022, 144, 5910-5920.	13.7	18
5	Training responsible engineers. Phronesis and the role of virtues in teaching engineering ethics. Australasian Journal of Engineering Education, 2021, 26, 25-37.	1.4	10
6	Mimicking the Electron Transport Chain and Active Site of [FeFe] Hydrogenases in One Metal–Organic Framework: Factors That Influence Charge Transport. Journal of the American Chemical Society, 2021, 143, 7991-7999.	13.7	25
7	Photoinduced Fano Resonances between Quantum Confined Nanocrystals and Adsorbed Molecular Catalysts. Nano Letters, 2021, 21, 5813-5818.	9.1	4
8	Ultrafast Dynamics in Cu-Deficient CuInS <sub>2</sub> Quantum Dots: Sub-Bandgap Transitions and Self-Assembled Molecular Catalysts. Journal of Physical Chemistry C, 2021, 125, 14751-14764.	3.1	9
9	Catalytic systems mimicking the [FeFe]-hydrogenase active site for visible-light-driven hydrogen production. Coordination Chemistry Reviews, 2021, 448, 214172.	18.8	38
10	Immobilising molecular Ru complexes on a protective ultrathin oxide layer of p-Si electrodes towards photoelectrochemical CO <sub>2</sub> reduction. Dalton Transactions, 2021, 50, 10482-10492.	3.3	9
11	Elemental Depth Profiling of Intact Metal–Organic Framework Single Crystals by Scanning Nuclear Microprobe. Journal of the American Chemical Society, 2021, 143, 18626-18634.	13.7	4
12	Using Surface Amide Couplings to Assemble Photocathodes for Solar Fuel Production Applications. ACS Applied Materials & Interfaces, 2020, 12, 4501-4509.	8.0	11
13	Selfâ€Recovery of Photochemical H 2 Evolution with a Molecular Diiron Catalyst Incorporated in a UiOâ€66 Metal–Organic Framework. ChemPhotoChem, 2020, 4, 287-290.	3.0	7
14	Analysis of electrocatalytic metal-organic frameworks. Coordination Chemistry Reviews, 2020, 406, 213137.	18.8	77
15	Synthetic strategies to incorporate Ru-terpyridyl water oxidation catalysts into MOFs: direct synthesis <i>vs.</i> post-synthetic approach. Dalton Transactions, 2020, 49, 13753-13759.	3.3	7
16	E,Z-Selectivity in the reductive cross-coupling of two benzaldehydes to stilbenes under substrate control. Organic and Biomolecular Chemistry, 2020, 18, 6171-6179.	2.8	1
17	Enhancing photovoltages at p-type semiconductors through a redox-active metal-organic framework surface coating. Nature Communications, 2020, 11, 5819.	12.8	15
18	Transport Phenomena: Challenges and Opportunities for Molecular Catalysis in Metal–Organic Frameworks. Journal of the American Chemical Society, 2020, 142, 11941-11956.	13.7	74

#	Article	IF	CITATIONS
19	Understanding the Performance of NiO Photocathodes with Alkyl-Derivatized Cobalt Catalysts and a Push–Pull Dye. ACS Applied Materials & Interfaces, 2020, 12, 31372-31381.	8.0	16
20	Diagnosing surface <i>versus</i> bulk reactivity for molecular catalysis within metal–organic frameworks using a quantitative kinetic model. Chemical Science, 2020, 11, 7468-7478.	7.4	7
21	The Fascinating World of Phosphanylphosphonates: From Acetylenic Phosphaalkenes to Reductive Aldehyde Couplings. Synlett, 2019, 30, 1867-1885.	1.8	6
22	Electrocatalytic Hydrogen Evolution from a Cobaloxime-Based Metal–Organic Framework Thin Film. Journal of the American Chemical Society, 2019, 141, 15942-15950.	13.7	135
23	Facile Orientational Control of M2L2P SURMOFs on ⟠100⟩ Silicon Substrates and Growth Mechanism Insights for Defective MOFs. ACS Applied Materials & Interfaces, 2019, 11, 38294-38302.	8.0	14
24	Elucidating Proton-Coupled Electron Transfer Mechanisms of Metal Hydrides with Free Energy- and Pressure-Dependent Kinetics. Journal of the American Chemical Society, 2019, 141, 17245-17259.	13.7	30
25	Post synthetic exchange enables orthogonal click chemistry in a metal organic framework. Dalton Transactions, 2019, 48, 45-49.	3.3	17
26	Direct Spectroscopic Detection of Key Intermediates and the Turnover Process in Catalytic H 2 Formation by a Biomimetic Diiron Catalyst. Chemistry - A European Journal, 2019, 25, 11135-11140.	3.3	10
27	Structural features of molecular electrocatalysts in multi-electron redox processes for renewable energy – recent advances. Sustainable Energy and Fuels, 2019, 3, 2159-2175.	4.9	31
28	Triarylalkenes from the site-selective reductive cross-coupling of benzophenones and aldehydes. Chemical Communications, 2019, 55, 6030-6033.	4.1	7
29	Restricted rotation of an Fe(CO) <sub>2</sub> (PL <sub>3</sub> )-subunit in [FeFe]-hydrogenase active site mimics by intramolecular ligation. Dalton Transactions, 2019, 48, 5933-5939.	3.3	13
30	Triphenylphosphaalkenes in Chemical Equilibria. European Journal of Inorganic Chemistry, 2019, 2019, 1562-1566.	2.0	8
31	Mechanistic insights on the non-innocent role of electron donors: reversible photocapture of CO <sub>2</sub> by Ru <sup>II</sup> -polypyridyl complexes. Dalton Transactions, 2019, 48, 16894-16898.	3.3	6
32	Uio-Type Metal-Organic Framework Thin Film with Redox-Active Linkers: Development and Charge Transport Behavior. ECS Meeting Abstracts, 2019, , .	0.0	0
33	Uio-Type Metal-Organic Framework Thin Film with Redox-Active Linkers: Development and Charge Transport Behavior. ECS Meeting Abstracts, 2019, , .	0.0	0
34	Development of a UiO-Type Thin Film Electrocatalysis Platform with Redox-Active Linkers. Journal of the American Chemical Society, 2018, 140, 2985-2994.	13.7	113
35	Self-Quenching and Slow Hole Injection May Limit the Efficiency in NiO-Based Dye-Sensitized Solar Cells. Journal of Physical Chemistry C, 2018, 122, 13902-13910.	3.1	11
36	Light-driven hydrogen evolution catalyzed by a cobaloxime catalyst incorporated in a MIL-101(Cr) metal–organic framework. Sustainable Energy and Fuels, 2018, 2, 1148-1152.	4.9	36

#	Article	IF	CITATIONS
37	Rapid Microwave-Assisted Self-Assembly of a Carboxylic-Acid-Terminated Dye on a TiO <sub>2</sub> Photoanode. ACS Applied Energy Materials, 2018, 1, 202-210.	5.1	3
38	New Talent: Europe, 2018. Dalton Transactions, 2018, 47, 10319-10319.	3.3	2
39	Accelerating proton-coupled electron transfer of metal hydrides in catalyst model reactions. Nature Chemistry, 2018, 10, 881-887.	13.6	78
40	Direct evidence of catalyst reduction on dye and catalyst co-sensitized NiO photocathodes by mid-infrared transient absorption spectroscopy. Chemical Science, 2018, 9, 4983-4991.	7.4	21
41	One-Pot Intermolecular Reductive Cross-Coupling of Deactivated Aldehydes to Unsymmetrically 1,2-Disubstituted Alkenes. Organic Letters, 2018, 20, 5086-5089.	4.6	13
42	Formal water oxidation turnover frequencies from MIL-101(Cr) anchored Ru(bda) depend on oxidant concentration. Chemical Communications, 2018, 54, 7770-7773.	4.1	18
43	Reductive coupling of two aldehydes to unsymmetrical <i>E</i> -alkenes <i>via</i> phosphaalkene and phosphinate intermediates. Chemical Communications, 2018, 54, 7163-7166.	4.1	10
44	Isolating the Effects of the Proton Tunneling Distance on Proton-Coupled Electron Transfer in a Series of Homologous Tyrosine-Base Model Compounds. Journal of the American Chemical Society, 2017, 139, 2090-2101.	13.7	48
45	Hydrogen evolution with nanoengineered ZnO interfaces decorated using a beetroot extract and a hydrogenase mimic. Sustainable Energy and Fuels, 2017, 1, 69-73.	4.9	35
46	Catalyst accessibility to chemical reductants in metal–organic frameworks. Chemical Communications, 2017, 53, 3257-3260.	4.1	42
47	Unsymmetrical <i>E</i> -Alkenes from the Stereoselective Reductive Coupling of Two Aldehydes. Journal of the American Chemical Society, 2017, 139, 2940-2943.	13.7	23
48	Characterization of compositional modifications in metal-organic frameworks using carbon and alpha particle microbeams. Nuclear Instruments & Methods in Physics Research B, 2017, 404, 198-201.	1.4	2
49	[FeFe] Hydrogenase active site model chemistry in a UiO-66 metal–organic framework. Chemical Communications, 2017, 53, 5227-5230.	4.1	27
50	Uniform distribution of post-synthetic linker exchange in metal–organic frameworks revealed by Rutherford backscattering spectrometry. Chemical Communications, 2017, 53, 6516-6519.	4.1	27
51	Evaluation of two- and three-dimensional electrode platforms for the electrochemical characterization of organometallic catalysts incorporated in non-conducting metal–organic frameworks. Dalton Transactions, 2017, 46, 4907-4911.	3.3	17
52	Electronic and molecular structure relations in diiron compounds mimicking the [FeFe]-hydrogenase active site studied by X-ray spectroscopy and quantum chemistry. Dalton Transactions, 2017, 46, 12544-12557.	3.3	8
53	Homogeneous Water Oxidation by Half‣andwich Iridium(III) Nâ€Heterocyclic Carbene Complexes with Pendant Hydroxy and Amino Groups. ChemSusChem, 2017, 10, 4616-4623.	6.8	20
54	Asymmetric Cyclometalated Ru <sup>II</sup> Polypyridyl-Type Complexes with π-Extended Carbanionic Donor Sets. Inorganic Chemistry, 2017, 56, 7720-7730.	4.0	7

#	Article	IF	CITATIONS
55	Electrocatalytic water oxidation by a molecular catalyst incorporated into a metal–organic framework thin film. Dalton Transactions, 2017, 46, 1382-1388.	3.3	79
56	Hydrogen Bonded Phenolâ€Quinolines with Highly Controlled Protonâ€Transfer Coordinate. European Journal of Organic Chemistry, 2016, 2016, 3365-3372.	2.4	5
57	Direct, Sequential, and Stereoselective Alkynylation of <i>C,C</i> â€Dibromophosphaalkenes. Chemistry - A European Journal, 2016, 22, 10614-10619.	3.3	12
58	Activating a Low Overpotential CO <sub>2</sub> Reduction Mechanism by a Strategic Ligand Modification on a Ruthenium Polypyridyl Catalyst. Angewandte Chemie - International Edition, 2016, 55, 1825-1829.	13.8	78
59	Tuning the Electronic Properties of Acetylenic Fluorenes by Phosphaalkene Incorporation. Chemistry - A European Journal, 2016, 22, 4247-4255.	3.3	18
60	Iron Pentapyridyl Complexes as Molecular Water Oxidation Catalysts: Strong Influence of a Chloride Ligand and pH in Altering the Mechanism. ChemSusChem, 2016, 9, 1178-1186.	6.8	57
61	Photochemical Hydrogen Production with Metal–Organic Frameworks. Topics in Catalysis, 2016, 59, 1712-1721.	2.8	34
62	Judicious Ligand Design in Ruthenium Polypyridyl CO <sub>2</sub> Reduction Catalysts to Enhance Reactivity by Steric and Electronic Effects. Chemistry - A European Journal, 2016, 22, 14870-14880.	3.3	35
63	Dynamics and Photochemical H <sub>2</sub> Evolution of Dye–NiO Photocathodes with a Biomimetic FeFe-Catalyst. ACS Energy Letters, 2016, 1, 1106-1111.	17.4	70
64	Ultrafast Electron Transfer Between Dye and Catalyst on a Mesoporous NiO Surface. Journal of the American Chemical Society, 2016, 138, 8060-8063.	13.7	60
65	Activating a Low Overpotential CO <sub>2</sub> Reduction Mechanism by a Strategic Ligand Modification on a Ruthenium Polypyridyl Catalyst. Angewandte Chemie, 2016, 128, 1857-1861.	2.0	22
66	The potential of ion beams for characterization of metal–organic frameworks. Nuclear Instruments & Methods in Physics Research B, 2016, 371, 327-331.	1.4	3
67	Synthesis of the first metal-free phosphanylphosphonate and its use in the "phospha–Wittig–Horner― reaction. Dalton Transactions, 2016, 45, 2201-2207.	3.3	20
68	Cooperative Gold Nanoparticle Stabilization by Acetylenic Phosphaalkenes. Angewandte Chemie - International Edition, 2015, 54, 10634-10638.	13.8	15
69	What Limits Photon Upconversion on Mesoporous Thin Films Sensitized by Solution-Phase Absorbers?. Journal of Physical Chemistry C, 2015, 119, 4550-4564.	3.1	28
70	Concerted proton-coupled electron transfer from a metal-hydride complex. Nature Chemistry, 2015, 7, 140-145.	13.6	88
71	Human ride comfort prediction of drive train using modeling method based on artificial neural networks. International Journal of Automotive Technology, 2015, 16, 153-166.	1.4	14
72	Water oxidation catalysed by a mononuclear Co <sup>II</sup> polypyridine complex; possible reaction intermediates and the role of the chloride ligand. Chemical Communications, 2015, 51, 13074-13077.	4.1	62

Sascha Ott

#	Article	IF	CITATIONS
73	Versatile Approach to 3-Phosphahexatrienes Bearing Low Coordinated Phosphorus. Phosphorus, Sulfur and Silicon and the Related Elements, 2015, 190, 638-646.	1.6	1
74	Watching the dynamics of electrons and atoms at work in solar energy conversion. Faraday Discussions, 2015, 185, 51-68.	3.2	10
75	The 6,6â€Dicyanopentafulvene Core: A Template for the Design of Electronâ€Acceptor Compounds. Chemistry - A European Journal, 2015, 21, 8168-8176.	3.3	13
76	Photon Upconversion from Chemically Bound Triplet Sensitizers and Emitters on Mesoporous ZrO <sub>2</sub> : Implications for Solar Energy Conversion. Journal of Physical Chemistry C, 2015, 119, 25792-25806.	3.1	27
77	Functionalization of robust Zr( <scp>iv</scp> )-based metal–organic framework films via a postsynthetic ligand exchange. Chemical Communications, 2015, 51, 66-69.	4.1	107
78	Structural dynamics inside a functionalized metal–organic framework probed by ultrafast 2D IR spectroscopy. Proceedings of the National Academy of Sciences of the United States of America, 2014, 111, 18442-18447.	7.1	76
79	Direct Observation of Key Catalytic Intermediates in a Photoinduced Proton Reduction Cycle with a Diiron Carbonyl Complex. Journal of the American Chemical Society, 2014, 136, 17366-17369.	13.7	49
80	Redox Switching in Ethenylâ€Bridged Bisphospholes. Chemistry - A European Journal, 2014, 20, 16083-16087.	3.3	11
81	Tuning the Optical Properties of 1,1′â€Biphospholes by Chemical Alterations of the P–P Bridge. European Journal of Inorganic Chemistry, 2014, 2014, 1760-1766.	2.0	11
82	1,4-Disilacyclohexa-2,5-diene: a molecular building block that allows for remarkably strong neutral cyclic cross-hyperconjugation. Chemical Science, 2014, 5, 360-371.	7.4	18
83	Coordination and conformational isomers in mononuclear iron complexes with pertinence to the [FeFe] hydrogenase active site. Dalton Transactions, 2014, 43, 4537-4549.	3.3	43
84	Mechanistic insights into electrocatalytic CO <sub>2</sub> reduction within [Ru <sup>II</sup> (tpy)(NN)X] <sup>n+</sup> architectures. Dalton Transactions, 2014, 43, 15028-15037.	3.3	57
85	Water Oxidation Catalyzed by a Dinuclear Cobalt–Polypyridine Complex. Angewandte Chemie - International Edition, 2014, 53, 14499-14502.	13.8	114
86	Enhanced Photochemical Hydrogen Production by a Molecular Diiron Catalyst Incorporated into a Metal–Organic Framework. Journal of the American Chemical Society, 2013, 135, 16997-17003.	13.7	501
87	Oxaphospholes and Bisphospholes from Phosphinophosphonates and α,βâ€Unsaturated Ketones. Chemistry - A European Journal, 2013, 19, 13692-13704.	3.3	19
88	Mechanism of the Phosphaâ€Wittig–Horner Reaction. Angewandte Chemie - International Edition, 2013, 52, 6484-6487.	13.8	23
89	Alternative Synthesis of A C,C-Diacetylenic Phosphaalkene. Phosphorus, Sulfur and Silicon and the Related Elements, 2013, 188, 164-167.	1.6	3
90	Toward Metathesis Reactions on Vinylphosphaalkenes. Phosphorus, Sulfur and Silicon and the Related Elements, 2013, 188, 152-158.	1.6	15

#	Article	IF	CITATIONS
91	Mechanism of the Phosphaâ€Wittig–Horner Reaction. Angewandte Chemie, 2013, 125, 6612-6615.	2.0	11
92	Mixed-valence [FeIFeII] hydrogenase active site model complexes stabilized by a bidentate carborane bis-phosphine ligand. Dalton Transactions, 2012, 41, 12468.	3.3	40
93	Alternative Synthesis and Structures of <i>C</i> â€monoacetylenic Phosphaalkenes. Zeitschrift Fur Anorganische Und Allgemeine Chemie, 2012, 638, 2219-2224.	1.2	19
94	Site-Selective X-ray Spectroscopy on an Asymmetric Model Complex of the [FeFe] Hydrogenase Active Site. Inorganic Chemistry, 2012, 51, 4546-4559.	4.0	28
95	Electronic Structure of an [FeFe] Hydrogenase Model Complex in Solution Revealed by X-ray Absorption Spectroscopy Using Narrow-Band Emission Detection. Journal of the American Chemical Society, 2012, 134, 14142-14157.	13.7	36
96	Light-Driven Electron Transfer between a Photosensitizer and a Proton-Reducing Catalyst Co-adsorbed to NiO. Journal of the American Chemical Society, 2012, 134, 19322-19325.	13.7	95
97	Cascade Reactions Forming Highly Substituted, Conjugated Phospholes and 1,2â€Oxaphospholes. Angewandte Chemie - International Edition, 2012, 51, 7776-7780.	13.8	18
98	Structural and spectroscopic characterization of tetranuclear iron complexes containing a bridge. Journal of Coordination Chemistry, 2012, 65, 2713-2723.	2.2	12
99	Photoelectrochemical Hydrogen Generation by an [FeFe] Hydrogenase Active Site Mimic at a <i>p</i> â€Type Silicon/Molecular Electrocatalyst Junction. Chemistry - A European Journal, 2012, 18, 1295-1298.	3.3	43
100	Ironing Out Hydrogen Storage. Science, 2011, 333, 1714-1715.	12.6	45
101	Pentacoordinate iron complexes as functional models of the distal iron in [FeFe] hydrogenases. Chemical Communications, 2011, 47, 11662.	4.1	55
102	Spectroscopically characterized intermediates of catalytic H2 formation by [FeFe] hydrogenase models. Energy and Environmental Science, 2011, 4, 2340.	30.8	130
103	Comparing the Reactivity of Benzenedithiolate- versus Alkyldithiolate-Bridged Fe2(CO)6 Complexes with Competing Ligands. European Journal of Inorganic Chemistry, 2011, 2011, 1106-1111.	2.0	33
104	Synthesis and IR Spectroelectrochemical Studies of a [60]Fulleropyrrolidineâ€(tricarbonyl)chromium Complex: Probing C <sub>60</sub> Redox States by IR Spectroscopy. European Journal of Inorganic Chemistry, 2011, 2011, 1744-1749.	2.0	8
105	Reductive Diphosphene Formation From W(CO)5-Coordinated Dichlorophosphanes. Phosphorus, Sulfur and Silicon and the Related Elements, 2011, 186, 664-665.	1.6	2
106	Directing protonation in [FeFe] hydrogenase active site models by modifications in their second coordination sphere. Chemical Communications, 2010, 46, 5775.	4.1	79
107	Highâ€Turnover Photochemical Hydrogen Production Catalyzed by a Model Complex of the [FeFe]â€Hydrogenase Active Site. Chemistry - A European Journal, 2010, 16, 60-63.	3.3	201
108	Introducing a dark reaction to photochemistry: photocatalytic hydrogen from [FeFe] hydrogenase active site model complexes. Dalton Transactions, 2009, , 9952.	3.3	122

#	Article	IF	CITATIONS
109	Biomimetic and Microbial Approaches to Solar Fuel Generation. Accounts of Chemical Research, 2009, 42, 1899-1909.	15.6	403
110	(I,0) Mixed-Valence State of a Diiron Complex with Pertinence to the [FeFe]-Hydrogenase Active Site: An IR, EPR, and Computational Study. Inorganic Chemistry, 2009, 48, 10883-10885.	4.0	57
111	Tuning the electronic properties of Fe2(μ-arenedithiolate)(CO)6â^'n(PMe3)n (n=0, 2) complexes related to the [Fe–Fe]-hydrogenase active site. Comptes Rendus Chimie, 2008, 11, 875-889.	0.5	127
112	Facilitated Hydride Binding in an Feâ^'Fe Hydrogenase Activeâ^'Site Biomimic Revealed by X-ray Absorption Spectroscopy and DFT Calculations. Inorganic Chemistry, 2007, 46, 11094-11105.	4.0	43
113	Bio-inspired, side-on attachment of a ruthenium photosensitizer to an iron hydrogenase active site model. Dalton Transactions, 2006, , 4599-4606.	3.3	105
114	Iron hydrogenase active site mimic holding a proton and a hydride. Chemical Communications, 2006, , 520-522.	4.1	154
115	Dynamic ligation at the first amine-coordinated iron hydrogenase active site mimic. Chemical Communications, 2006, , 4206-4208.	4.1	52
116	Iron hydrogenase active site mimics in supramolecular systems aiming for light-driven hydrogen production. Coordination Chemistry Reviews, 2005, 249, 1653-1663.	18.8	267
117	A Biomimetic Pathway for Hydrogen Evolution from a Model of the Iron Hydrogenase Active Site. Angewandte Chemie - International Edition, 2004, 43, 1006-1009.	13.8	232
118	Model of the Iron Hydrogenase Active Site Covalently Linked to a Ruthenium Photosensitizer:Â Synthesis and Photophysical Properties. Inorganic Chemistry, 2004, 43, 4683-4692.	4.0	136
119	Title is missing!. Angewandte Chemie, 2003, 115, 3407-3410.	2.0	39
120	Synthesis and Structure of a Biomimetic Model of the Iron Hydrogenase Active Site Covalently Linked to a Ruthenium Photosensitizer. Angewandte Chemie - International Edition, 2003, 42, 3285-3288.	13.8	191
121	Zâ€ʿselective alkene formation from reductive aldehyde homoâ€couplings. European Journal of Organic Chemistry, 0, , .	2.4	3